

# Modelled Behaviour of a High Temperature Electrolyser System Coupled with a Solar Farm

Floriane Petipas<sup>a,b</sup>, Annabelle Brisse<sup>a</sup>, Chakib Bouallou<sup>\*,b</sup>

<sup>a</sup>EIFER (European Institute for Energy Research), Emmy-Noether Str. 11, 76131 Karlsruhe, Germany

<sup>b</sup>MINES ParisTech, PSL Research University - Centre for Energy efficiency of Systems, 60 bd Saint Michel, 75006 Paris, France

chakib.bouallou@mines-paristech.fr

A system model was developed in Simulink® in order to describe the dynamic behaviour of HTE (High Temperature Electrolysis) systems fed with variable power. This model is composed of three coupled submodels focusing on the electrolyser, on the Balance of Plant and on the control strategies, respectively. The implemented control strategies ensure optimised operation in terms of both electrolysis material restrictions, such as thermal gradients, and system efficiency. The presented results were simulated for a standalone system composed of a four-unit electrolyser fed with electrical power from a virtual 1.35 MW solar farm in Marignane (France) and producing compressed hydrogen (3 MPa). A thermal insulation of 30 cm around each unit limits thermal losses, so the temperature drops by only 10 K overnight. Over the simulated year, the solar farm produced 2.76 GWh which were converted into 64.5 t of compressed hydrogen. The results show that HTE intermittent operation is technically feasible without an external heat source. Moreover, the system efficiency remains as high as 92 % based on the hydrogen Higher Heating Value (HHV) if suitable control strategies are employed.

## 1. Introduction

Since feeding Renewable Energy (RE) into the electrical grid causes technical problems due to the grid stability constraints, the deployment of large-scale energy-storage technologies is required to facilitate the RE market penetration. While storing large amounts of electrical energy is a challenge, storing large amounts of gas is not an issue. In this framework, the Power-to-Gas concept has a great potential (De Saint-Jean et al., 2014). The key element of this concept is the conversion of electricity into hydrogen, performed with an electrolyser which should be flexible, efficient and affordable for Power-to-Gas to become a cost-effective solution. The High Temperature Electrolyser (HTE) is highly efficient and has the potential to become affordable, through both lifetime increase and mass production. Nevertheless, no study of this technology operation under variable conditions has been reported so far. Yet, flexibility should be studied both at the materials level, to analyse the impact on the materials lifetime, and at the system level, to identify the influence on the HTE system behaviour and efficiency. This work focuses on HTE behaviour while fed with solar energy.

Most SOEC stack models found in the literature were one-dimensional models, describing the parameters evolution along the cell. The stack model of O'Brien et al. (2005) and more recently O'Brien et al. (2010) aimed to calculate the average Nernst voltage, cell operating voltage, gas outlet temperatures and electrolyser efficiency for any specified inlet gas flow rates, current density, cell active area, and external heat loss. For the calculation, Rivera-Tinoco et al. (2010) divided the cell length into small sections in which the cell voltage, gas flow rates and temperatures were calculated with an iterative method. In the operating range considered for practical operation, the calculated current density, voltage and temperature were quasi-linear along the cell (Udagawa et al., 2007) and more recently Rivera-Tinoco et al. (2010) in spite of both the complex one-dimensional calculation and the use of cell parameters which are difficult to estimate, such as the tortuosity. In this work, a one-dimensional model is therefore considered not to be required to describe SOEC systems.

Moreover, due to the lack of experimental data, white-box models (based on physical equations) are usually proposed. Overvoltages are then described in detail, based on the Butler-Volmer equation for the calculation of activation overvoltages, the Ohm's law for the calculation of the ohmic losses, and the Fick's law for the calculation of the concentration overvoltages. On the contrary, when experimental data are available, grey-box models (based on both physical equations and experimental data) can be proposed, which is the case of O'Brien et al. (2005) and later Fu et al. (2008) who both used expressions of the ASR as a function of the temperature derived from experimental data. Since grey-box zero-dimensional models exhibit fast computational time and accurate results for the degree of detail which is of interest for the SOEC system integration, this type of model would be adapted to this work.

## 2. SOEC system dynamic model

### 2.1 Model presentation

A dynamic system model that describes the behaviour of SOEC (Solid Oxide Electrolysis Cell) systems when fed with variable power was developed in Simulink<sup>®</sup>, which is data flow graphical programming software. This software was chosen because it enables developing parametric dynamic models based on the MATLAB<sup>®</sup> programming environment. To provide modularity and calculation speed, a parametric grey-box zero-dimensional model was chosen. The model is composed of two coupled submodels describing the electrolyser module and the Balance of Plant (BoP), respectively, as displayed in Figure 1. In order to compare the calculated system efficiency with typical low temperature electrolysis processes operating under pressure, no external heat source ( $T_{source} = 288$  K) is provided and the produced hydrogen is compressed from the atmospheric pressure to 3 MPa ( $p_{out}$ ).

Due to the high operating temperature, steam has to be provided to the electrolyser module. The corresponding heat requirements are covered in the balance of plant by an efficient recovery of the outlet gases heat and of the compression heat, as well as by electrical heating. The electrolyser module provides a behaviour description at the cell level, whereas the BoP module allows optimising the heat recovery. The detailed description of this model is explained by Petipas et al. (2013b).

The definition of the SOEC system hierarchy is very important for a clear understanding of the terms used in this work. In this paper, 278 SOE cells are assembled to form an SOEC stack, which is connected with 8 similar stacks to form an insulated SOEC unit composed of 9 stacks. Four units are connected to form one SOEC module. Finally, the combination of the SOEC module and the BoP module is called the SOEC system.

### 2.2 Dealing with variable power

As explained by Petipas et al., (2013c), the power range of the system is limited to 60 - 100 % if no control strategies are developed. The unit average temperature and efficiency are almost linear against the applied load. Around 60 % load, the unit runs in the endothermic mode, which leads to a lower average temperature and higher efficiency. Around 100 % load, the unit runs in the exothermic mode, which leads to a higher average temperature and lower efficiency.

Two control strategies are used in this study. The first strategy consists in switching off units when the unit power decreases below 60 % of the maximum power. The power is distributed among fewer units, which enables operating units to operate within their power range of 60 - 100 %. Moreover, when the power is very low, a complementary control strategy is deployed. Indeed, when the unit power decreases below the minimum unit power of 60 %, a unit heater is used to balance the thermal loss within the unit. The use of these control strategies enlarges the system power range from 60 - 100 % to 3 - 100 % of the maximum power. Concerning the intermittent operation, an experiment has shown that switching on and off an SOEC cell did not damage or reduce the performance of the cell (Petipas et al., 2013a). Thus we can make the assumption that an intermittent operation between the tolerated power range of 60 - 100 % and 0 % is not damageable for the SOEC cells.

## 3. Coupling with solar

### 3.1 Solar power data

For coupling of the SOEC system with solar power, the selected site is Marignane (Southern France), since very high irradiation is reported for this region. Both the irradiation and the ambient temperature are required to calculate the generated power. For this study, 2005 data are collected with a 10 min step for the irradiation from the SoDa services (SoDa) and with a 1-hour step for the temperature from the website Meteociel (Meteociel). The photovoltaic panels are fully dedicated to hydrogen production. A panel surface of 10 m<sup>2</sup> is assumed to provide a power of 1 kWp, therefore 13,500 m<sup>2</sup> of photovoltaic panels is required to match the maximum SOEC system power (around 1.35 MW). Figure 2 shows the solar power data used in

the model for a 1.35 MW SOEC system. Over one year, the cumulative energy produced by the 1.35 MW photovoltaic panels equals 2.76 GWh.

electrolyser module = 4 units

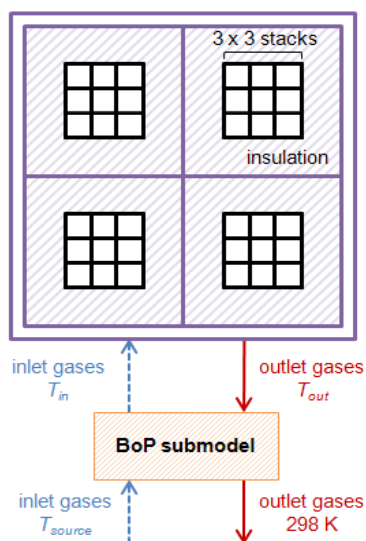


Figure 1: Scheme of the modelled configuration

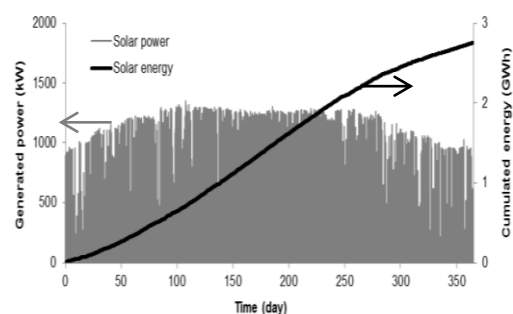


Figure 2: Generated solar power and cumulative energy over one year (2005), used as a model input.

### 3.2 Overall results of the Solar-SOEC system

As shown in Figure 3, the hydrogen production rate follows the solar power load curve. Three horizontal lines can be identified on the curve, at  $8 \text{ kg h}^{-1}$ ,  $14 \text{ kg h}^{-1}$  and  $19 \text{ kg h}^{-1}$ . These lines correspond to the unit switch. Therefore, for production rates of  $0-8 \text{ kg h}^{-1}$ ,  $8-14 \text{ kg h}^{-1}$ ,  $14-19 \text{ kg h}^{-1}$  and  $19-31.5 \text{ kg h}^{-1}$ , one, two, three and four units are operated respectively, following the first control strategy explained in Part 2.2.

These four zones noticeable in Figure 3 are due to perturbations when units start or stop operating. This is due to the change in the electrolyser operating mode (endothermic, exothermic). When an additional unit is started, the load per unit decreases thus the operating mode changes from the exothermic to the endothermic mode and the BoP consumption increases. Due to this increase, the power allocated to the electrolyser units decreases, thus one unit stops. When one unit stops, the load per unit increases thus the operating mode changes from the endothermic to the exothermic mode and the BoP consumption decreases. Due to this decrease, the power allocated to the electrolyser units increases, thus one unit starts. As long as the input power equals the “unit switching power”, the unit keeps starting and stopping. This phenomenon could be avoided by adjusting the modular control strategy, by introducing a “switching power range” instead of a “switching power value”. Since this work aims to validate the proposed control strategies and not to provide an accurate control of the system, this additional control strategy has not been integrated in this work.

The hydrogen production rate follows the photovoltaic power load curve. After one year, 64.5 tons of hydrogen are produced. The overall SOEC system efficiency equals therefore 92 % vs. HHV. The back-up power used to preheat the units when no power was available supplied 108 kWh, which was too low to impact on the system efficiency. As detailed in Figure 4, the system efficiency is not constant during dynamic operation because of the BoP consumption. Moreover, the system efficiency varies because of the switches between the endothermic and exothermic modes, related to the number of units in operation. Therefore, because of the daily frequency of the irradiation profile, the system efficiency varies also with a daily frequency, most values being in the range 85 - 95 % vs. HHV.

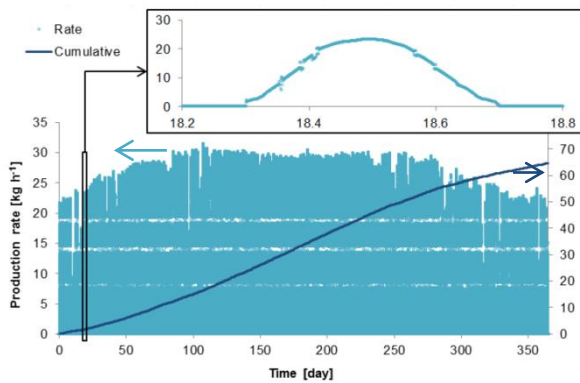


Figure 3: Solar hydrogen production evolution over one year.

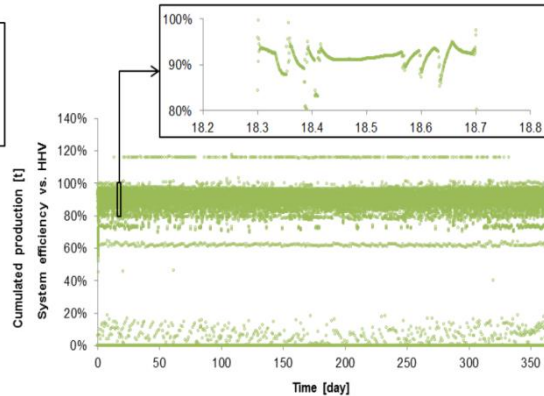


Figure 4: System efficiency evolution over one year.

### 3.3 Solar power distribution among the components

The input photovoltaic power is distributed among the electrolysis power and the BoP heater power which represent more than 90 % of the SOEC system consumption. The electrolysis power corresponds to the power fed to the SOEC stacks, without considering the power consumption of the unit heaters. With the control strategies employed, the SOEC system follows the load curve, including cold start-up ( $t = 0$  d), ramps (every day), short periods of standstill (every night) and long periods of standstill ( $t = 9 - 11$  d).

### 3.4 Modular operation of the Solar-SOEC system

Due to the solar quasi-continuous profile, unit 1 absorbs the base load, whereas units 2 and 3 absorb intermediate load and unit 4 shaves the load peak. Therefore, the cumulative hydrogen production is much higher for unit 1 (23.2 t), than for the other units (respectively 17.3, 13.5 and 10.6 t). The average hydrogen production per unit equals therefore  $16 \pm 7$  t.

When looking into detail in the power distribution among units (Figure 5), the phenomenon of base load, intermediate load and load peak absorption is clearer. However, unit 1 additionally follows the solar power intermittency, whereas other units operate around the thermoneutral mode. As a consequence, since unit 1 follows the load curve, it is put in standby only 370 times over one year, whereas other units are put in standby around 2,000 times, which corresponds to around 5 electric on-off cycles per day. Below 57 % load, units 2, 3 and 4 do not operate, although power values can be observed in Figure 5. These power values below 57 % were actually cached during a unit switch.

Concerning the temperature, numerous thermal cycles in the operating range 1,023 - 1,123 K are observed. Decreases below 1,023 K are detected 366 times for unit 1 and around 300 times for other units over one year. Decreases below 923 K did not occur for units 1 and 2, and occurred only once and twice for units 3 and 4. No decrease below 833 K occurred, therefore, the units were always either operated under pure steam, or in standby above 1023 K or in shut down above 833 K, both under a mixture of hydrogen and steam. A nitrogen purge was never necessary since the temperature did not decrease below 833 K.

### 3.5 Intermittency and standby of the Solar-SOEC system

Results show a clear daily frequency which is due to the power ramp up and down, implying an operation in the endothermic and exothermic modes within the day, depending on the number of operating units. At night, all units are in standby (above 1,023 K) or shut-down (between 833 K and 1,023 K). The longest period of standstill over the year is shown in Figure 6, where the solar power is low for a few days. As a consequence, unit 1 operates daily and is in standby mode overnight, which causes a temperature decrease of 20 K per night. Since unit 1 usually operates below 57 % load in the late afternoon, the temperature equals 1,023 K. The temperature decrease below 1,023 K overnight implies a shut-down, which does not impact on the gas concentrations. In the morning, a short heat-up is required to reach 1,023 K again.

When the solar power is low, other units are most of the time in standby or shut-down, depending on the temperature. Unit 4 is stopped from  $t = 13.6$  to  $t = 18.4$  d. During this standstill period, the temperature decreased from 1,066 K to 911 K. This decrease by only 155 K is important to notice because it implies both little heat-up energy and little heat-up time when the unit needs to be operated again.

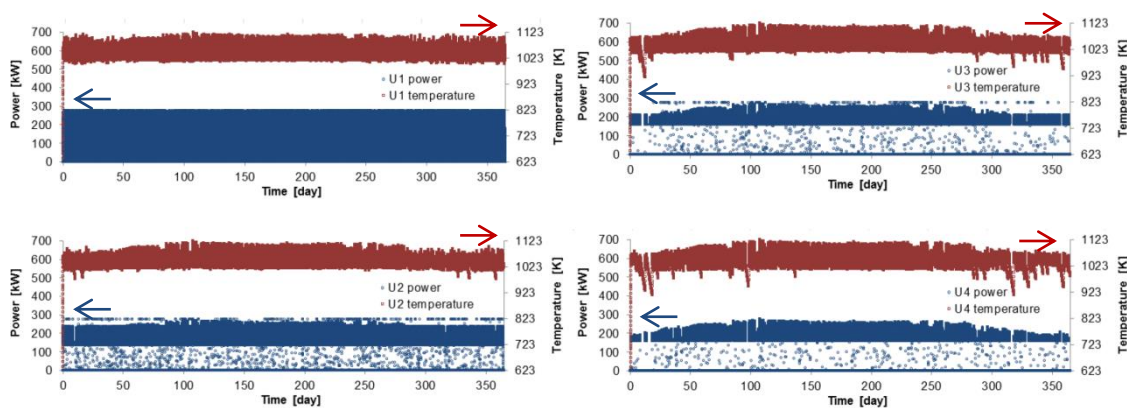


Figure 5: Electrolysis power and average temperature evolutions of each unit.

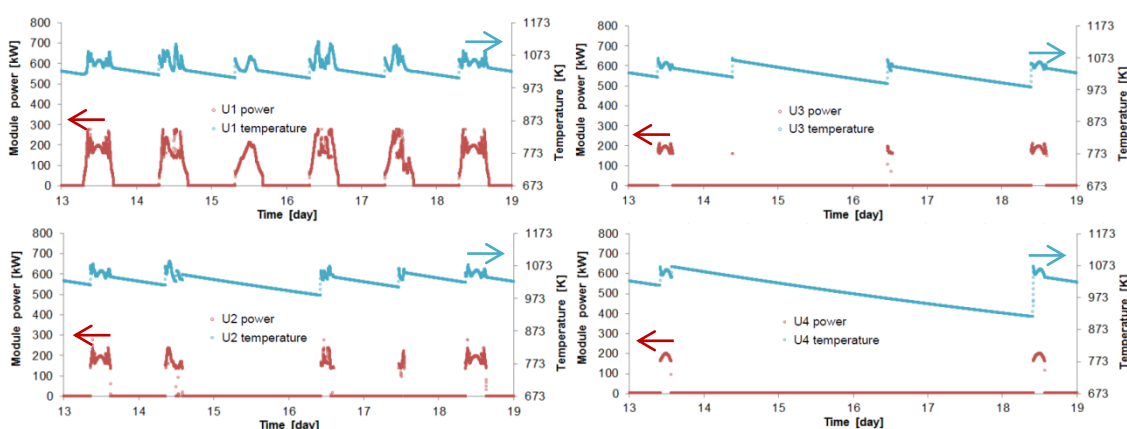


Figure 6: Electrolysis power and average temperature evolutions during the longest standstill period.

### 3.6 Cold start-up of the Solar-SOEC system

Concerning the cold start-up phase, again due to the solar ramp profile, units are not heated up simultaneously but one after the other, as displayed in Figure 7.

Heat-up of unit 1 starts at  $t = 6.63$  h (0.276 d) for unit 1 to be operated at 7.37 h (0.307 day). Since the solar power rises, heat-up of unit 2 starts at  $t = 7.95$  h (0.332 d) for unit 2 to be operated at 8.72 h (0.363 d). At  $t = 8.80$  h (0.367 d), unit 3 is heated and operates at  $t = 9.56$  h (0.398 d). At  $t = 9.63$  h (0.401 d), unit 4 is heated and starts operate at  $t = 10.38$  h (0.433 d). The units start being heated up 43 min before they need to be operated. Therefore the cold start-up begins at different times for each unit. On these curves, the principle of modular operation appears clearly.

## 4. Conclusion

This paper aimed to show the SOEC system behaviour under dynamic operating conditions, through the case study of a fictive Solar SOEC system. The SOEC system was dimensioned to match the maximum generated power (1.35 MW), which corresponds to a standalone system configuration. In spite of intermittent variations, the system efficiency over one year was 92 % vs. HHV, which shows that the SOEC system integrating the proposed control strategies is adapted to various uses. Moreover, the number of on-off electric cycles was 5-7 per day and per unit, which is unlikely to degrade the units, apart from the first unit, which followed the load profile and was put in standby once a day on average. Finally, the issue related to thermal transients has been solved with the use of a thick insulation. Indeed, the temperature mostly cycled within the range 1,023 - 1,123 K, which corresponds to the operating temperature range and is not damageable for the stack materials. Decreases below 1,023 K occurred for each unit on average once a day. It is important to notice that no decrease below 833 K occurred over the whole year, although the temperature was only maintained through thermal insulation in standby and shut down modes.

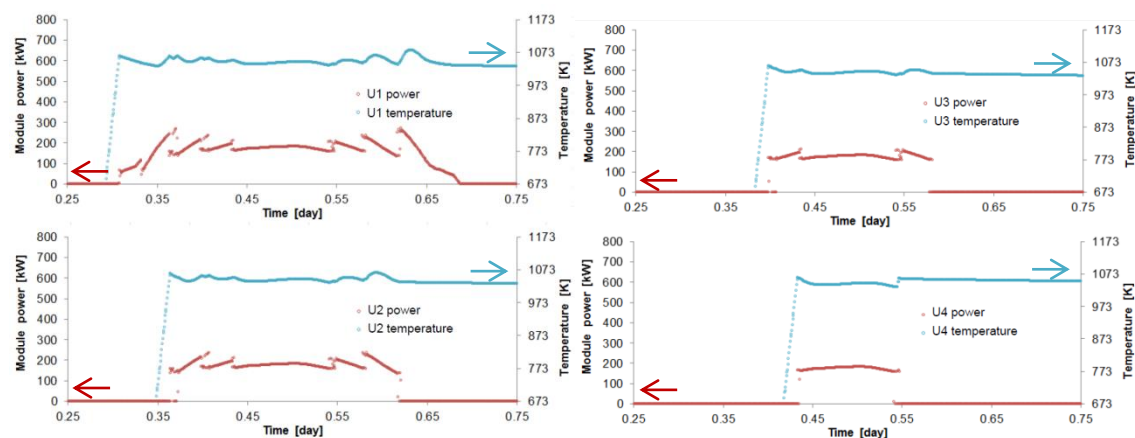


Figure 7: Cold start-up electrolysis power and average temperature evolutions.

## References

- De Saint Jean M., Baurens P., Bouallou C., 2014, Study of the efficiency of a HT power to gas process, *Chemical Engineering Transactions*, 39, 391-396.
- European Communities, 2006, Photovoltaic Solar Electricity Potential in European Countries <[www.climacare.dk/userfiles/file/Dokumenter/Solindfald%20i%20Europa.pdf](http://www.climacare.dk/userfiles/file/Dokumenter/Solindfald%20i%20Europa.pdf)> accessed 15.01.2015.
- Meteociel, Table of hourly weather observations <[www.meteociel.fr/temps-reel/obs\\_villes.php](http://www.meteociel.fr/temps-reel/obs_villes.php)> accessed 15.01.2015.
- Fu Q., Mabilat C., Zahid M., Brisse A., Gautier L., 2010, Syngas production via high-temperature steam/CO<sub>2</sub> co-electrolysis: an economic assessment, *Energy and Environmental Science*, 3, 1382-1397.
- O'Brien J.E., Stoots C.M., Hawkes G.L., 2005, Comparison of a one-dimensional model of a High-Temperature Solid-Oxide Electrolysis stack with CFD and experimental results. Proceedings of the 2005 ASME International Mechanical Engineering Congress, Orlando, USA.
- O'Brien J.E., McKellar M.G., Harvego E.A., Stoots C.M., 2010, High-temperature electrolysis for large-scale hydrogen and syngas production from nuclear energy - summary of system simulation and economic analyses, *International Journal of Hydrogen Energy*, 35, 4808-4819.
- Petipas F., Fu Q., Brisse A., Bouallou C., 2013a, Transient operation of a solid oxide electrolysis cell, *International Journal of Hydrogen Energy*, 38, 2957-2964.
- Petipas F., 2013b, Design and control of high temperature electrolyser systems fed with renewable energies, PhD thesis, MINES ParisTech, Paris, France.
- Petipas F., Brisse A., Bouallou C., 2013c, Model-based behaviour of a high temperature electrolyser system operated at various loads, *Journal of Power Sources*, 23, 584-595.
- Rivera-Tinoco R., Mansilla C., Bouallou C., 2010, Competitiveness of hydrogen production by High Temperature Electrolysis: Impact of the heat source and identification of key parameters to achieve low production costs, *Energy Conversion and Management*, 51(12), 2623-2634.
- SoDa (Solar Energy Services for Professionals), Time Series of Solar Radiation Data <[www.soda-is.com/eng/services/services\\_radiation\\_free\\_eng.php](http://www.soda-is.com/eng/services/services_radiation_free_eng.php)> accessed 15.01.2015
- Udagawa J., Aguiar P., Brandon N.P., 2007, Hydrogen production through steam electrolysis: Model-based steady state performance of a cathode-supported intermediate temperature solid oxide electrolysis cell, *Journal of Power Sources*, 166, 127-136.